Journal of Engineering Science and Technology Review 16 (2) (2023) 59 - 65

Research Article

JOURNAL OF
Engineering Science and Technology Review

www.jestr.org

Constitutive Model of Water Immersion Damage to Cement Stabilized Macadam under Water Weak Effect and Uniaxial Compression

Baoxing Gong[1], Zhanyou Yan[1,*] and Chunliu Li[2]

[1]*College of Civil Engineering, Shijiazhuang Tiedao University, Shijiazhuang 050043, China*
[2]*Institute of Urban Construction, Hebei Normal University of Science & Technology, Qinhuangdao 066004, China*

Received 11 January 2023; Accepted 28 March 2023

Abstract

To reveal the damage mechanism of cement-stabilized macadam, the mechanical properties of cement-stabilized aggregates immersed in water for different times were examined by uniaxial compression tests, and the evolution of damage factors of cement-stabilized aggregates specimens was investigated. On the basis of theory of Weibull distribution, the material constitutive relationship suitable for the destruction of cement-stabilized macadam materials immersed in water was proposed. Results show that the strength/elastic modulus of cement-stabilized macadam decreases with the increase in immersion time in water, indicating that water has a weakening effect on cement-stabilized macadam. Linear/nonlinear phases appear in the stress-strain curve. The influence of shape parameters on nonpore compression stage is greater than that on pore compression stage. The damage variable remains constant in the early stage. The stress-strain curve of the damage model is in good agreement with that of the test data. The conclusions obtained in this study provide a significant reference for cement-stabilized macadam engineering.

Keywords: Cement stabilized macadam, Uniaxial compression, Immersion softening, Damage factor

1. Introduction

Since the high compressive strength of aggregate at the early stage of subgrade formation, it is commonly used as a load-bearing layer in the structural design of high-grade bituminous pavements in China. The main raw materials of the pavement are soil, stone, and industrial waste. Aggregate has wide sources of accessible, low-cost raw materials and simple construction process, thus providing it with significant technical and economic advantages [1-3]. It is an important pavement structural linkage layer, since the cement-stabilized aggregates play an important role in ensuring the load-bearing capacity, stability, and durability of the pavement structure. However, the cement-stabilized aggregates encounter many problems, such as loosening, interface slippage, cracks, and water damage during the course of application under various environmental factors, construction techniques, construction equipment, and traffic loads, causing great losses to the society and economy.

To investigate the damage evolution of cement-stabilized aggregates, many scholars studied the damage mechanism under different working conditions using various methods, such as flushing, dissolution, and loading and unloading. The obtained results have solved many construction problems [4]. However, due to the wide distribution of monsoon climate in China and the high pressure of highway traffic, the water damage problem of pavement subgrade has become prominent. As the main material of high-grade highway subgrade, the cement-stabilized aggregates exhibit water softening when immersed in water for a long time. With the extension of soaking time, the peak load stress, elastic modulus, and other conventional mechanical parameters that cement-stabilized aggregates can withstand will be seriously reduced. Current investigations failed to reveal the performance deterioration law of cement-stabilized aggregates under water immersion conditions. In addition, theoretical and experimental support for the construction and optimization of the damage model of cement-stabilized aggregates is lacking.

Therefore, it is of great significance to extend the service life of cement-stabilized aggregates subgrade and the design of pavement structure by simulating the actual road base material with water immersion and analyze the damage mechanism of cement-stabilized aggregates material structure.

2. State of the art

Some scholars have studied the cement composite materials [5-7]. Tasnimi et al. [8] proposed a new constitutive relation to study the nonlinear mechanical behavior of cement concrete construction. On basis of the damage variables and fracture parameters of the specimen under compression, the same principle holds true for the specimen under tension. When constructing the damage model of cement concrete, Darabi et al. [9] added some nonlinear damage models into the damage model. The healing effect of material microdamage was considered, and the variation of damage density was analyzed. Under axial and cyclic lateral loads, Kenawy et al. [10] proposed a uniaxial nonlocal constitutive model that could accurately predict the local deformation of concrete structures based on damage mechanics and plasticity theory. When analyzing the damage characteristics of cement mixture, Zhang and Oeser [11] regarded fatigue failure as residual strength degradation. Combining with the continuum damage model, they constructed the residual strength model of the phenomenological damage evolution theory and verified that by experiments. Using the damage

*E-mail address: yanzahnyou@163.com
ISSN: 1791-2377
doi:10.25103/jestr.162.08

function to simulate the energy storage function, Lanzoni and Tarantino [12] established the relationship between material constitution and energy release rate based on the continuum and thermodynamic theory and then derived the dominant expression from the value of the equilibrium edge. To analyze the damage of cement mixture, Tan et al. [13] established the structural damage model according to the energy theory and they found the consistency between material damage and energy dissipation. In addition, the ratio of lime to sand was proportional to the energy reserve of material.

Lemaitre [14] established a mean continuous–isotropic plastic damage model based on effective stress and proved the linear relationship between structural damage and equivalent strain by experiments. To accurately simulate the fracture of concrete, Abu Al-Rub and Kim [15] proposed an isotropic/anisotropic damage coupling model based on the continuity hypothesis and damage mechanics. Breccolotti et al. [16] established a concrete damage model by optimizing structural damage, which was suitable for structural fatigue. Doherty and Muir [17] proposed a constitutive model that could reflect the weak cementing particles in cement mixture through the mechanical relationship of weak cementing materials and they analyzed the transient curing of cement mixture in specific environments. The damage of low temperature to cement concrete structures has been considered in several studies [18-22]. Under sulfate addition, the damage constitutive model of cement concrete was built and the damage mechanism of cement concrete was analyzed [23-26].

For the weakening of cement-stabilized crushed stone, it is commonly used as the pavement base. This phenomenon is directly regarded as linear compression in the early and middle nonlinear stages in uniaxial compression test (stress-strain curve) of cement-stabilized macadam. Meanwhile, the pore and microcracks within the specimen itself are ignored. When early pore compression stage is directly ignored, it will cause a large error in the research of cement concrete damage when the damage mechanism of cement-stabilized macadam is analyzed from the meso perspective.

In this study, different immersion tests of cement-stabilized macadam were first carried out. The stress-strain curve was obtained by the uniaxial compression test. The unit strength of meso-particles in cement-stabilized macadam was assumed to conform to Weibull distribution [27]. The stress-strain curve including the early pore compression and the late nonpore compression was constructed based on statistical damage mechanics theory. The size parameters and shape parameters of the damage model were obtained by experiments. The damage variables of water to cement-stabilized macadam under different immersion conditions were analyzed. The simulation data were compared with the experimental data. Finally, a damage model of cement-stabilized macadam under water weakening effect was proposed.

The rest of this study is organized as follows. Section 3 introduces the specimen preparation and damage model of water weakening and uniaxial compression. Section 4 analyzes the simulation and test results, and finally, the conclusions are summarized in Section 5.

3. Methodology

3.1 Specimen preparation

The cement-stabilized macadam specimens were prepared in accordance with the standard of Chinese Test Code for The Stability of Inorganic Binder in Highway Engineering (JTG E51-2009). The specimen is a standard cylinder of Φ150 mm × 150 mm. The material composition of the specimens is listed in Table 1. After reaching the curing age, the prepared standard specimen was kept in an area of ventilation and dryness for 30 d to reduce the influence of high moisture content on the test during the curing period. Finally, the intact specimens were selected for immersion test (Fig. 1). Firstly, the lower quarter of the specimen was immersed in water for 2 h. Water was then added to the lower half of the specimen, followed by immersion for another 2 h. Water was added again, and the lower 3/4 of the specimen was immersed in water for 2 h. Finally, water was continuously added until the whole specimen was immersed in water, and immersion was performed for the time required for the test. The specimens were immersed in water for 3, 7, 15, 20, 25, and 30 d, respectively.

Table. 1. Particle distribution of test pieces.

Particle size (mm)	0-5	5-10	10-20	20-25
Percentage (%)	32	19	35	14

Fig. 1. Specimens immersed in steps.

3.2 Damage model of water weakening and uniaxial compression

3.2.1 Constitutive relationship of damage coupling

According to the theory of damage mechanics, the damage degree of specimen is usually expressed by the change of contact area and damage factor D_n. When the specimen is damaged, the contact area of the cementing material between the aggregates in the specimen will inevitably decrease, which is denoted by $A-\bar{A}$. The ratio of $A-\bar{A}$ to the original total contact area A is the damage factor as follows:

$$D_n = \frac{A-\bar{A}}{A} \tag{1}$$

where, A is the total contact area of the cementing material between particles. $\bar{A}$ is the contact area between particles after the damage of cementitious material.

When $D_n = 0$, the specimen was in the undamaged state. When $D_n = 1$, the specimen has been eventual failure. When $0 < D_n < 1$, the specimen was in the damaged state.

According to the relationship between damage factor, elastic modulus E_0 and effective strain ε_e, effective stress $\bar{\sigma}$ could be shown as follows [13]:

$$\bar{\sigma} = \frac{\sigma}{1-D} = E_0 \varepsilon_e \tag{2}$$

According to Eq. 2, the basic mechanical relationship of continuous damage is:

$$\sigma_t = E_0\left(1-D_t\right)\varepsilon_e \tag{3}$$

According to the principle of equivalent strain, the effective strain produced by the effective stress in the first damage state to the second damage state is equal to the effective stress in the second damage state on the first damage state. The stress under different damage states can be obtained as follow:

$$\sigma = E_0\left(1-D_W\right)\varepsilon \tag{4}$$

$$\sigma = E_t\left(1-D_l\right)\varepsilon \tag{5}$$

According to phenomenological damage mechanics, the damage factor induced by water weakening can be defined as follows:

$$D_t = 1-\frac{E_t}{E_0} \tag{6}$$

where, E_t is the elastic modulus after the immersed for time t, and E_0 is the elastic modulus in dry state. D_l is the damage variable caused by uniaxial compression, D_t is the damage variable caused by immersion for t d, and D_W is the total damage variable.

According to Eqs. 3 to 6, the total damage of specimen produced by water weakening and uniaxial compression, could be obtained in Eq. 7.

$$D_W = D_l + D_t - D_l D_t \tag{7}$$

3.2.2 Optimization of damage model

The internal particles of cement stabilized macadam aggregate are randomly distributed from microscopic view. The strength of the meso-particle element conforms to Weibull distribution [27]. According to statistical damage mechanics theory, the probability density function of damaged particles could be shown as follow:

$$P(\varepsilon) = \frac{m}{\eta}\left(\frac{\varepsilon}{\eta}\right)^{m-1} \mathrm{e}^{-\left(\frac{\varepsilon}{\eta}\right)^m} \tag{8}$$

where, η and m respectively represented scale parameters and shape parameters, which can reflect the response characteristics of the specimen, and they are non-negative values. ε represents the strain of the specimen.

When the specimen was loaded to time t, the strain generated is ε. The microdamage $P(x)\mathrm{d}x$ generated in the interval $\left[\varepsilon, \varepsilon + \mathrm{d}\varepsilon\right]$ and the total contact N of the particles inside the specimen can be regarded as the total damage of the specimen. So, the microdamage that has been generated is $\int_0^{\varepsilon} NP(x)\mathrm{d}x$. When the strength damage is subject to Weibull, the damage variable can be obtained as follows:

$$D_l = \frac{\int_0^{\varepsilon} NP(x)\mathrm{d}x}{N} = 1 - e^{-\left(\frac{\varepsilon}{\eta}\right)^m} \tag{9}$$

According to Eqs. 3 to 5 and Eq. 9, the total damage variable formed by the combined action of water weakening and uniaxial compression can be obtained as follows:

$$D_w = 1-\frac{E_t}{E_0}\mathrm{e}^{-\left(\frac{\varepsilon}{\eta_t}\right)^{m_t}} \tag{10}$$

The constitutive relation can be obtained as follows:

$$\sigma = E_t\varepsilon\mathrm{e}^{-\left(\frac{\varepsilon}{\eta_t}\right)^{m_t}} \tag{11}$$

When the stress-strain curve of the uniaxial compression test after the specimen is immersed in water is analyzed, the pore compression of the specimen was defined as the early nonlinear stage, so the stress-strain curve is treated in sections.

$$\sigma = \begin{cases} E_t\varepsilon\left[1-\mathrm{e}^{-\left(\frac{\varepsilon}{\eta_{1,t}}\right)^{m_{1,t}}}\right] & \left(\varepsilon \le \varepsilon_A\right) \\ E_t\left(\varepsilon-\varepsilon_{c,t}\right)e^{-\left(\frac{\varepsilon-\varepsilon_A}{\eta_{2,t}}\right)^{m_{2,t}}} + \sigma_A & \left(\varepsilon > \varepsilon_A\right) \end{cases} \tag{12}$$

The initial stage of uniaxial compression is called the first stage. At the first stage, with the increasing load, the pores of the specimen were constantly compressed. The initial cracks in the specimen were compacted and the pore volume was reduced. There were no visible cracks at first stage. According to the theory of damage mechanics, this stage is usually regarded as no damage.

$$D_w = \begin{cases} 1-\frac{E_t}{E_0} & \left(\varepsilon \le \varepsilon_A\right) \\ 1-\frac{E_t}{E_0}e^{-\left(\frac{\varepsilon-\varepsilon_A}{\eta_{2,t}}\right)^{m_{2,t}}} & \left(\varepsilon > \varepsilon_A\right) \end{cases} \tag{13}$$

where, η_t and m_t respectively represent the scale and shape parameters of the distribution function at the t time of immersion.

The mechanical relation in the stress-strain curve can be shown as follows:

$$\begin{cases} \varepsilon = 0\ ,\ \sigma = 0 \\ \varepsilon = \varepsilon_A\ ,\ \sigma = \sigma_A \\ \varepsilon = \varepsilon_A\ ,\ \frac{\mathrm{d}\sigma}{\mathrm{d}\varepsilon} = E \\ \varepsilon = \varepsilon_{max}\ ,\ \sigma = \sigma_{max} \\ \varepsilon = \varepsilon_{max}\ ,\ \frac{\mathrm{d}\sigma}{\mathrm{d}\varepsilon} = 0 \end{cases} \tag{14}$$

When the stress reaches the maximum value, the relationship between stress and immersion time can be shown as follows:

$$\sigma\big|_{\varepsilon=\varepsilon_{max}} = E_t\left(\varepsilon_{max}-\varepsilon_A\right)e^{-\left(\frac{\varepsilon_{max}-\varepsilon_A}{\eta_{2,t}}\right)^{m_{2,t}}} + \sigma_A = \sigma_{max} \tag{15}$$

At the peak point, the stress is differentiated, Eq. 15 could be generalized as follows:

$$\frac{d\sigma}{d\varepsilon}\bigg|_{\varepsilon=\varepsilon_{max}} = E_t e^{-\left(\frac{\varepsilon_{max}-\varepsilon_A}{\eta_{2,t}}\right)^{m_{2,t}}} \times \left[1-\left(\varepsilon_{max}-\varepsilon_A\right)\frac{m_{2,t}}{\eta_{2,t}}\left(\frac{\varepsilon_{max}-\varepsilon_A}{\eta_{2,t}}\right)^{m_{2,t}-1}\right]=0 \tag{16}$$

In the stage of nonpore compression, when the strain is greater than $\varepsilon_{A,t}$, the size and shape parameters can be derived from Eqs. 15 and 16, as shown in Eq. 17.

$$m_{2,t} = \frac{1}{ln\left[\frac{E_t\left(\varepsilon_{max}-\varepsilon_A\right)}{\sigma_{max}-\sigma_A}\right]} \tag{17}$$

$$\eta_{2,t} = \left(\varepsilon-\varepsilon_A\right)m_{2,t}^{\frac{1}{m_{2,t}}} \tag{18}$$

At the end of the pore compression phase, the pores are compacted. The stress σ_A can be generalized as follows:

$$\sigma\big|_{\varepsilon=\varepsilon_A} = E_t\varepsilon_A\left[1-e^{-\left(\frac{\varepsilon_A}{\eta_{1,t}}\right)^{m_{1,t}}}\right]=\sigma_A \tag{19}$$

When the stress is differentiated, the expression of elastic modulus can be obtained as follows:

$$\frac{d\sigma}{d\varepsilon}\bigg|_{\varepsilon=\varepsilon_A} = -E_t e^{-\left(\frac{\varepsilon_A}{\eta_{1,t}}\right)^{m_{1,t}}}\left[1-\varepsilon_A\frac{m_{1,t}}{\eta_{1,t}}\left(\frac{\varepsilon_A}{\eta_{1,t}}\right)^{m_{1,t}-1}\right] = -E_t e^{-\left(\frac{\varepsilon_{p,t}-\varepsilon_A}{\eta_{2,t}}\right)^{m_{2,t}}}\left[1-\left(\varepsilon_{p,t}-\varepsilon_A\right)\frac{m_{1,t}}{\eta_{1,t}}\left(\frac{\varepsilon_{p,t}-\varepsilon_A}{\eta_{1,t}}\right)^{m_{2,t}-1}\right]=E_t \tag{20}$$

The shape parameter and scale parameter in the stage of pore compression can be shown as follows:

$$m_{1,t} = \left(1-\frac{1}{1-\frac{\sigma_A}{\varepsilon_A E_t}}\right)/\ln\left(1-\frac{\sigma_A}{\varepsilon_A E_t}\right) \tag{21}$$

$$\eta_{1,t} = \varepsilon_A\left[-\ln\left(1-\frac{\sigma_A}{\varepsilon_A E_t}\right)\right]^{-\frac{1}{m_{1,t}}} \tag{22}$$

4. Results analysis and discussion

4.1 Uniaxial compression test of cement stabilized macadam after water weakening

4.1.1 Analysis of stress-strain curve

In the uniaxial compression test of cement-stabilized macadam material, the classical linear stress-strain curve is shown in Fig. 2. The four main stages are observed. When the strain reaches ε_A, the stress reaches σ_A in OA segment, which is the stage of pore compression. With the increase in load, the strain and slope of the specimen gradually increase. As the slope increases to a certain point, the slope tends to stabilize at this point. The slope is nonlinear at this stage. AB is the linear compression stage. The stress-strain curve increases linearly, and the slope is E_t. When the strain reaches ε_B, it enters the BC segment, which is the nonlinear compression stage, during which the slope of the curve begins to decrease. The rate of stress decreases and the plastic deformation increases when the strain increases. When the stress–strain curve reaches its maximum value, it enters the final stage of compression failure, which is the CD segment. As the strain increases, the stress decreases rapidly, leading to failure.

Uniaxial compression tests were conducted on cement-stabilized macadam with different immersion times, and the stress-strain curves obtained are shown in Fig. 3.

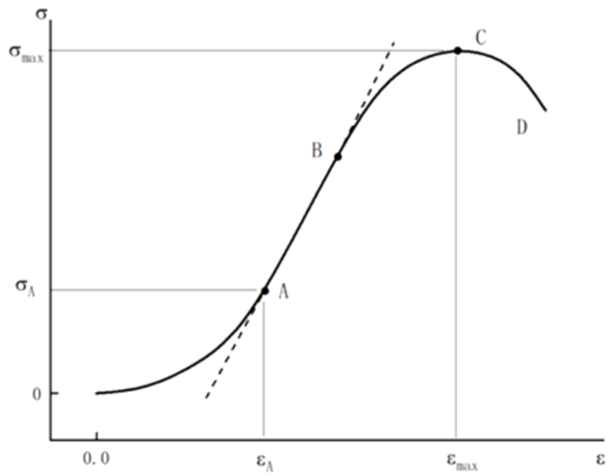

Fig. 2. Typical stress-strain curves of cement stabilized crushed stone specimens under uniaxial compression.

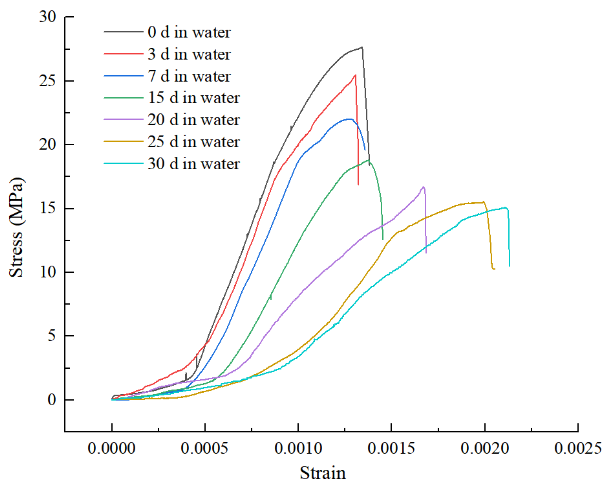

Fig. 3. Stress-strain curves of uniaxial compression tests at different immersion times.

As shown in Fig. 3, the dry specimen has the maximum peak strength and can withstand the maximum stress. With the increase in immersion time, the compressive strength gradually decreases. The variation of the stress-strain curve can be divided into four stages. The first stage is pore compression stage. The stress increases slowly when the strain increases. After the tiny pores in the specimen are gradually compacted, the aggregate is gradually stressed. In the second stage, the stress-strain curve is approximately linear with a fixed slope during the loading of cement-stabilized macadam specimen. In the third stage, the plastic deformation of the specimen increases. With the increase in strain, the stress shows a slowly increasing trend. In the fourth stage, the stress reaches a peak and then decreases rapidly. The maximum stress of the dry specimen is 27.67 MPa. After 30 d of immersion, the maximum compressive stress is 15.11 MPa, a reduction of about 45.38%.

In the uniaxial compression test of cement-stabilized macadam, microcracks are mainly generated along the vertical direction (Fig. 4). As the loading time increases, the crack continues to grow vertically. Cracks mostly occur in the middle of the specimen. A dynamic strain gauge was pasted on the flat surface of the specimen (Fig. 5) to test the vertical strain in the uniaxial compression test.

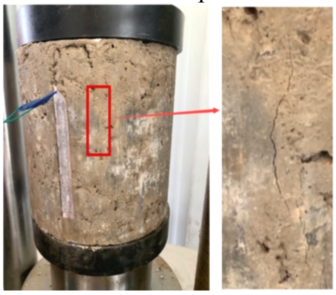

Fig. 4. Microcracks during uniaxial compression.

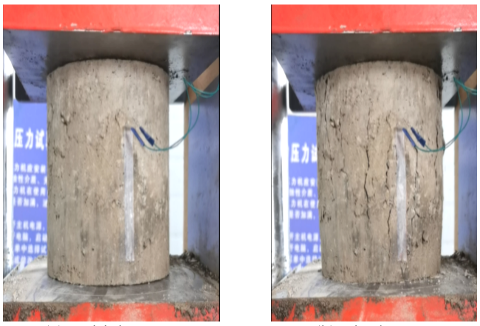

(a) Initial stage (b) Final stage

Fig. 5. Initial and final stages of specimen compression.

4.1.2 Parameter variation under water weakness effect

The peak stress variation curve of cement-stabilized macadam under different immersion conditions is shown in Fig. 6. The close relationship between the peak value of the maximum stress and the time of immersion can be described by the following formula:

$$\sigma_c = 10.18229 + \frac{17.51941}{1+\left(\frac{t}{13.53874}\right)^{1.22743}} \tag{23}$$

According to the variation rule of immersion time and stress peak, the maximum stress decreases rapidly with the increase in immersion time at 0-7 d and the curve is almost linear. After 7-20 d of immersion, the maximum stress decreases slowly and the curve shows a nonlinear trend.

The changing curve of elastic modulus of cement-stabilized macadam under different immersion conditions is shown in Fig. 7. At 0-7 d, the elastic modulus of cement-stabilized macadam decreases with prolonged immersion time. At 7-20 d, the elastic modulus of cement-stabilized macadam decreases at a relatively high rate.

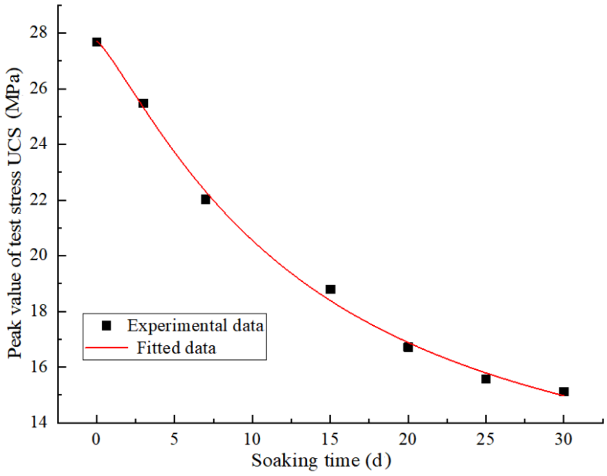

Fig. 6. Fitting curve of peak stress.

The formula of elastic modulus of specimen and immersion time can be expressed as:

$$E = -4.2527 + \frac{43.15787}{1+\left(\frac{t}{22.20814}\right)^{1.81106}} \tag{24}$$

4.2 Analysis of damage evolution

When the specimens were immersed in water for different times, the size parameters and shape parameters of cement-stabilized macadam materials could be solved (Table 2) according to the damage mechanics theory and uniaxial compression test. M_(1,t) and M_(2,t) represent the curve shape parameters in the stages of pore compression and nonpore compression, respectively. The shape parameters range from 1.083 to 1.526 in the pore compression stage and from 2.681 to 5.739 in the nonpore compression stage. The influence of nonpore compression stage on the shape parameters is greater than that of the pore compression stage.

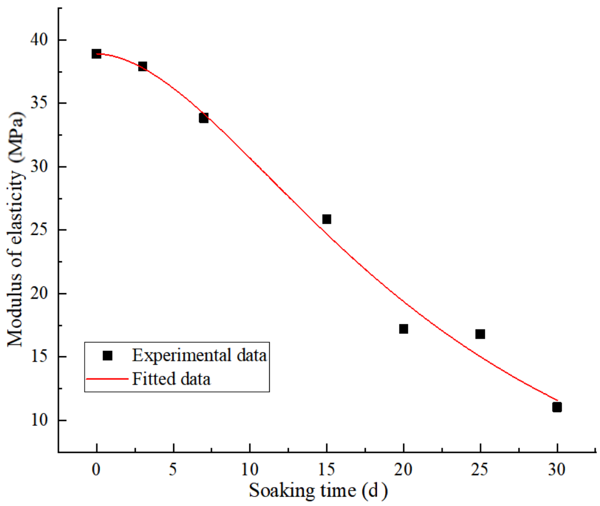

Fig. 7. Fitting curve of elastic modulus.

With the increase in immersion time, the elastic modulus of cement-stabilized macadamia decreases with values between 38.90 and 11.04 MPa. The peak stress of uniaxial compression test is between 27.67 and 15.11 MPa, and the corresponding strain is between 0.0013 and 0.0021. The relationship between the total loss of cement-stabilized macadam and the strain under different immersion conditions is shown in Fig. 8.

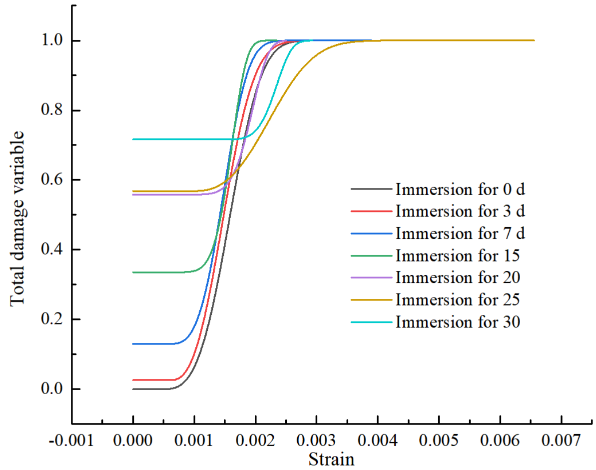

Fig. 8. Relationship between total damage variable and strain.

In the early stage of uniaxial compression, damage variables remain constant (due to water weakening) as shown in Fig. 8. When the load continues to increase, the strain and total damage of the specimen increase sharply (due to uniaxial compression). Finally, the damage variable of the specimen reaches 1. Owing to the water weakening effect, the damage variables reach 0, 0.026, 0.130, 0.336, 0.558, 0.568, and 0.716 after 0, 3, 7, 15, 20, 25, and 30 d of immersion, respectively. The longer the immersion time, the greater the damage variable and the strain of the specimen due to water weakening. The damage from being immersed in water for 20 d has exceeded 0.5.

4.3 Comparison of experimental and simulation data

The shape parameter m and scale parameter η of the early and late pore compression stages of the damage model were obtained through theoretical calculation (Table 2). The stress-strain curves of different immersion time can be obtained by substituting the calculated results into the stress-strain formulas of different stages. The stress-strain curves of the test and simulation figures are shown in Fig. 9.

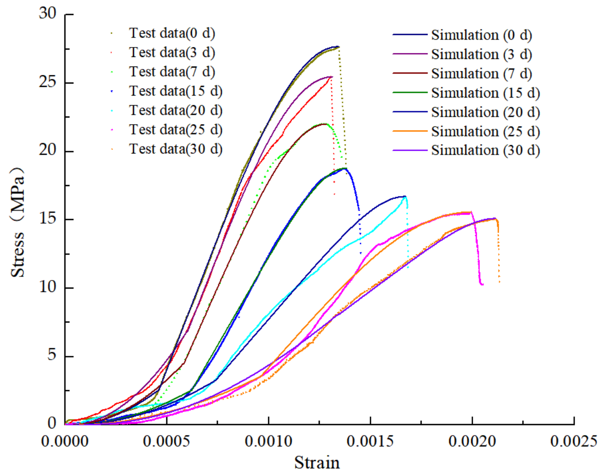

Fig. 9. Comparison of test stress-strain curve and simulation data.

The data of the theoretical calculation model is in good agreement with that of the test. With regard to the pore compression stage of the specimen, the damage accuracy of cement-stabilized macadam can be improved.

Table 2. Parameters of the experimental model.

Immersion time (d)	Test data (MPa)					Theoretical calculation			
	E_t	ε_{Pt}	σ_{Pt}	ε_{ct}	σ_{ct}	$m_{1,t}$	$\eta_{1,t}$	$m_{2,t}$	$\eta_{2,t}$
						Pore compression stage $\varepsilon \leq \varepsilon_A$		Non-pore compression stage $\varepsilon > \varepsilon_A$	
0	38.90	0.0013	27.67	0.0005	2.601	1.0828	0.0025	3.2085	0.0013
3	37.90	0.0013	25.48	0.0006	6.867	1.2048	0.0014	2.6807	0.0010
7	33.84	0.0013	22.03	0.0006	4.45	1.1416	0.0019	3.2804	0.0010
15	25.85	0.0014	18.80	0.0006	2.57	1.0926	0.0031	5.2358	0.0010
20	17.19	0.0017	16.71	0.0007	3.33	1.1673	0.0021	5.7392	0.0013
25	16.80	0.0020	15.58	0.0010	3.58	1.1366	0.0032	2.7146	0.0015
30	11.04	0.0021	15.11	0.0013	8.07	1.5257	0.0016	5.1549	0.0011

5. Conclusions

Water immersion test of cement-stabilized macadam was carried out in this study. The macroscopic mechanical characteristics of the specimens were tested in uniaxial compression test. The effect of water weakening on cement stabilized macadam was determined. The main conclusions were obtained as following:

(1) The strength and elastic modulus of cement-stabilized macadam are influenced by water immersion. The longer the immersion of cement-stabilized macadam in water, the greater the decrease in strength and elastic modulus. This finding shows that water has a weakening effect on cement-stabilized macadam. The linear/nonlinear phases appear in the stress-strain curve.

(2) The influence on shape parameters in the nonpore compression stage is greater than that in the pore compression stage. The value of damage variable of water to cement-stabilized macadam remains constant in the early stage but increases sharply in the later stage. The damage variable has exceeded 0.5 after 20 d of immersion. The longer the immersion time, the greater the damage variable. When the strain reaches 0.004, the value of each damage variable becomes close to 1, that is, the water weakening effect on cement-stabilized gravel is large.

(3) The initial damage of the specimen is mainly caused by water weakening and uniaxial compression. The parameters of the damage model can be obtained by uniaxial compression test. The stress-strain curve of the damage model is in good agreement with the test data.

This work only performed uniaxial compression experiments and simulation analysis of cement-stabilized aggregates under different soaking times. The subsequent studies can analyze the damage patterns of the specimens under different surrounding pressures on the basis of the current results.

Acknowledgements
This work was financially supported by the Science & Technology Program of Hebei (21375407D), China.

References

1. Monismith, C.L., Coetzee, N.E., "Reflection cracking: analysis, laboratory state and design considerations". *Journal of the Association of Asphalt Paving Technologt*, 49, 1980, pp. 268-313.
2. Jiwon, K., William, G.B., "Analysis of reflective crack control system involving reinforcing grid over base-isolating interlayer mixture". *Journal of Transportation Engineering*, 128(4), 2002, pp. 375-384.
3. George, K.P., "Mechanism of shrinkage cracking of soil-cement bases". *Highway Research Record*, (442), 1973, pp. 1-10.
4. Solonenko I., "The use of cement concrete pavements for roads, depending on climatic conditions". *Technical Journal*, 13(3), 2019, pp. 235-240.
5. Wu, X.G., Wang, S.R., Yang, J.H., Zhu, S., Kodama, J.I., "Mechanical properties and dynamic constitutive relation of lightweight shale ceramsite concrete". *European Journal of Environmental and Civil Engineering*, 26(7), 2022, pp. 2898-2912.
6. Xu, P., Cui, Y.H., Dai, J.F., Wang, S.R., Zhang, M.X., Hou, Z.G. "Mechanical performance of texttile reinforced concrete containing steel fibers and basalt fibers dubjected to high temperatures". *Ceramics-Silikáty*, 65 (3), 2021, pp. 263-272.
7. Wang, S.R., Zhao, J.Q., Gong, J., Xu, J.M., Li, C.L., "Analysis on energy absorption capacity of MLWC under electromagnetic driving SHPB condition". *DYNA*, 30(1), 2023, pp. 256-264.
8. Tasnimi, A.A., Lavasani, H.H., "Uniaxial constitutive law for structural concrete members under monotonic and cyclic loads". *Scientia Iranica*, 18(2), 2011, pp. 150-162.
9. Darabi, M.K., Rashid, Al-Rub, R.K.A., Masad, E.A., Little, D.N., "Constitutive modeling of fatigue damage response of asphalt concrete materials". *Transportation Research Record*, 2373(1), 2013, pp. 11-21.
10. Kenawy, M., Kunnath, S., Kolwankar, S., Kanvinde, A., "Concrete uniaxial nonlocal damage-plasticity model for simulating post-peak response of reinforced concrete beam-columns under cyclic loading". *Journal of Structural Engineering*, 146(5), 2020, pp. 04020052.
11. Zhang, Z., Oeser, M., "Residual strength model and cumulative damage characterization of asphalt mixture subjected to repeated loading". *International Journal of Fatigue*, 135, 2020, pp. 105534.
12. Lanzoni, L., Tarantino, A.M., "Equilibrium configurations and stability of a damaged body under uniaxial tractions". *Zeitschrift fürangewandte Mathematik und Physik*, 66(1), 2015, pp. 171-190.
13. Tan, Y.L., Gu, Q.H., Ning, J.G., Liu, X.S., Jia, Z.C., Huang, D.M., "Uniaxial compression behavior of cement mortar and its damage-constitutive model based on energy theory". *Materials*, 12(8), 2019, pp. 1309.
14. Lemaitre, J., "A continuous damage mechanics model for ductile fracture". *Transactions of the Asme Journal of Engineering Materials & Technology*, 107(1), 1985, pp. 83-89.
15. Abu Al-Rub, R.K., Kim, S.M., "Computational applications of a coupled plasticity-damage constitutive model for simulating plain concrete fracture". *Engineering Fracture Mechanics*, 77(10), 2010, pp. 1577-1603.
16. Breccolotti, M., Bonfigli, M.F., D'Alessandro, A., Materazzi, A.L., "Constitutive modeling of plain concrete subjected to cyclic uniaxial compressive loading". *Construction and Building Materials*, 94, 2015, pp. 172-180.
17. Doherty, J.P., Muir W.D., "A bonding and damage constitutive model for lightly cemented granular material". *Computers and Geotechnics*, 127, 2020, pp. 103732.
18. Yi, S.T., Pae, S.W., Kim, J.K., "Minimum curing time prediction of early-age concrete to prevent frost damage". *Construction and Building Materials*, 25(3), 2010, pp. 1439-1449.
19. Cwirzen, A., Sztermen, P., Habermehl-Cwirzen, K., "Effect of baltic seawater and binder type on frost durability of concrete". *Journal of Materials in Civil Engineering*, 26(2), 2014, pp. 298-287.
20. Tikkanen, J., Cwirzen, A., Penttala, V., "Freeze–thaw resistance of normal strength powder concretes". *Magazine of Concrete Research*, 67(2), 2015, pp. 71-81.
21. Porras, Y., Jones, C., Schmiedeke, N., "Freezing and thawing durability of high early strength portland cement concrete". *Journal of Materials in Civil Engineering*, 32(5), 2020, pp. 04020077.
22. Yang, D.Y., Luo, J.J., "The damage of concrete under flexural loading and salt solution". *Construction and Building Materials*, 36, 2012, pp. 129-134.
23. Zhang, J.S., Zhang, Y.H., Feng, L.P., Jin, D.B., Wang, C.C., Dong, Q.Y., "Damage model of fresh concrete in sulphate environment". *Journal of Central South University*, 22(3), 2015, pp. 1104-1113.
24. Wu, X.G., Wang, S.R., Yang, J.H., Zhao, J.Q., Chang, X., "Damage characteristics and constitutive model of lightweight shale ceramsite concrete under static-dynamic loading". *Engineering Fracture Mechanics*, 259, 2022, pp. ID 108137.
25. Sun, X.M., He, M.C., Liu, C.Y., Gu, J.C., Wang, S.R., Ming, Z.Q., Jing, H.H., "Development of nonlinear triaxial mechanical experiment system for soft rock specimen". *Chinese Journal of Rock Mechanics and Engineering*, 24(16), 2005, pp. 2870-2874.
26. Wang, S.R., Shi, K.P., Zou, Y.F., Zou, Z.S., Wang, X.C., Li, C.L., "Size effect analysis of scale test model for high-speed railway foundation under dynamic loading condition". *Tehnicki Vjesnik-Technical Gazette*, 28(5), 2021, pp. 1615-1625.
27. Weibull, W., "A statistical distribution function of wide applicability". *Journal of Applied Mechanics*, 18(3), 1951, pp. 293-297.